Science of the Total Environment 949 (2024) 174768

Contents lists available at ScienceDirect

Science of the Total Environment

journal homepage: www.elsevier.com/locate/scitotenv

Reduced bioavailability of Au and isotopically enriched ^{109}Ag nanoparticles transformed through a pilot wastewater treatment plant *in Hyalella azteca* under environmentally relevant exposure scenarios

Sebastian Kuehr [a,*], Ralf Kaegi [b], Johannes Raths [c,d], Brian Sinnet [b], Marco Kipf [b], Mark Rehkämper [e], Karl Andreas Jensen [f], Ralph A. Sperling [g], Kuria Ndungu [a], Anastasia Georgantzopoulou [a]

[a] Norwegian Institute for Water Research, Oslo, Norway
[b] Department of Process Engineering, Swiss Federal Institute of Aquatic Science and Technology Eawag, Dübendorf, Switzerland
[c] Department of Environmental Chemistry, Swiss Federal Institute of Aquatic Science and Technology Eawag, Dübendorf, Switzerland
[d] Institute of Biogeochemistry and Pollutant Dynamics, ETH Zürich, Zürich, Switzerland
[e] Department of Earth Science & Engineering, Imperial College London, London, UK
[f] Norwegian University of Life Science, Ås, Norway
[g] Fraunhofer Institute for Microengineering and Microsystems IMM, Mainz, Germany

HIGHLIGHTS

- Isotopically enriched ^{109}Ag and Au nanoparticles (NP) were spiked to a pilot wastewater treatment plant (WWTP).
- Exposure of aquatic invertebrates at environmentally realistic conditions for availability assessment
- Isotopic enrichment allowed to track NPs fate in WWTP matrices and exposed amphipods against high background.
- Reduced uptake of ^{109}Ag and Au after the NP passed through a WWTP
- Brackish exposure conditions alone reduce the uptake of pristine NP.

GRAPHICAL ABSTRACT

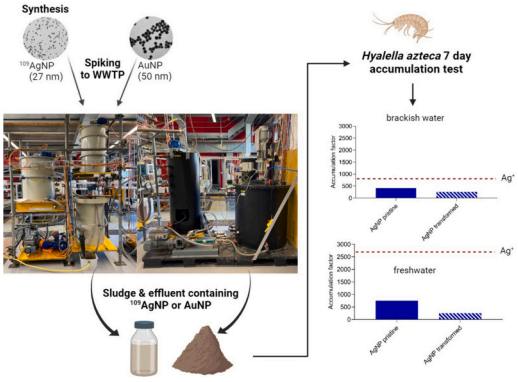

ARTICLE INFO

Editor: Damia Barcelo

Keywords:
Wastewater treatment plant
Nanoparticles
Environmental transformation
Isotopic enrichment
Bioavailability
Hyalella azteca

ABSTRACT

Wastewater Treatment Plants (WWTP) are a major repository and entrance path of nanoparticles (NP) in the environment and hence play a major role in the final NP fate and toxicity. Studies on silver nanoparticles (AgNP) transport via the WWTP system and uptake by aquatic organisms have so far been carried out using unrealistically high AgNP concentrations, unlikely to be encountered in the aquatic environment. The use of high AgNP concentrations is necessitated by both the low sensitivity of the detection methods used and the need to distinguish background Ag from spiked AgNP.

In this study, isotopically enriched ^{109}AgNP were synthesized to overcome these shortcomings and characterized by a broad range of methods including transmission electron microscopy, dynamic and electrophoretic

* Corresponding author.
E-mail address: Sebastian.kuehr@niva.no (S. Kuehr).

https://doi.org/10.1016/j.scitotenv.2024.174768
Received 15 April 2024; Received in revised form 21 June 2024; Accepted 11 July 2024
Available online 14 July 2024

light scattering. ^{109}AgNP and gold NP (AuNP) were spiked to a pilot wastewater treatment plant fed with municipal wastewater for up to 21 days. AuNP were used as chemically less reactive tracer. The uptake of the pristine and transformed NP present in the effluent was assessed using the benthic amphipod *Hyalella azteca* in fresh- and brackish water exposures at environmentally relevant concentrations of 30 to 500 ng Au/L and 39 to 260 ng Ag/L. The unique isotopic signature of the ^{109}AgNP allowed to detect the material at environmentally relevant concentrations in the presence of a much higher natural Ag background. The results show that the transformations reduce the NP uptake at environmentally relevant exposure concentrations. For ^{109}Ag, lower accumulation factors (AF) were obtained after exposure to transformed NP (250–350) compared to the AF values obtained for pristine ^{109}AgNP (750–840). The reduced AF values observed for *H. azteca* exposed to effluent from the AuNP-spiked WWTP indicate that biological transformation processes (e.g. eco-corona formation) seem to be involved in addition to chemical transformation.

1. Introduction

The increasing production and use of nanomaterials (NM) inevitably leads to an increased release into the environment (Nowack and Bucheli, 2007; Gottschalk and Nowack, 2011; Sun et al., 2017; Rajput et al., 2020). Markus et al. reported for 2013 that in the Netherlands alone 46 mg of silver nanoparticles (AgNP) per person, as one of the most produced NM, are released yearly into the wastewater (Markus et al., 2013). By this, it is not surprising that between 2014 and 2018 AgNP concentrations of up to 2.1 (Norway), 2.2 (Sweden) and 3.3 μg/L (UK) were measured in the wastewater entering wastewater treatment plants (WWTPs) (Johnson et al., 2014; Östman et al., 2017; Polesel et al., 2018). According to Mahapatra et al. (2015), in the USA alone, an estimated 1.3 t of gold nanoparticles (AuNP) from pharmaceutical use entered the sewage system in 2015 (Mahapatra et al., 2015).

Even though the majority of NM form hetero-agglomerates with the biomass during the activated treatment and accumulate in the sludge, a small fraction of NM still reaches the aquatic environment through the WWTP effluent. Due to this, the main entry path of NM into the environment is via wastewater and finally through the WWTP matrices such as sludge and effluent (Kaegi et al., 2011; Lowry et al., 2012). Once NM are in contact with wastewater they are subjected to physicochemical transformations, such as sulfidation, hetero-agglomeration, dissolution and biomolecule binding, which can alter their physicochemical properties and influence their behavior and fate. For AgNP in particular, these transformations have been well studied, especially in the context of the WWTP process (Kaegi et al., 2011; Lowry et al., 2012; Kaegi et al., 2013; Ma et al., 2014).

Due to the altered physicochemical properties, both pristine and transformed NM should be considered for more realistic exposure scenarios and (eco-)toxicological studies to avoid over or underestimation of potential hazard. Although few studies have addressed this issue by using transformed NM in exposure and effect studies some limitations exist, due to the use of artificial effluents, the application of artificial or chemical ageing methods for the NP, or the use of high NM concentrations to overcome the high background concentrations of elements of interest in the wastewater (Muth-Köhne et al., 2013; Kühr et al., 2018; Hartmann et al., 2019; Zeumer et al., 2020a; Hund-Rinke et al., 2021; Georgantzopoulou et al., 2020; Georgantzopoulou et al., 2018; Poynton et al., 2019).

In the current study, isotopically enriched AgNP (^{109}AgNP) were synthesized allowing to trace them despite the high background of Ag in the wastewater (Benn and Westerhoff, 2008) and in the organisms. A pilot WWTP operating with municipal wastewater was spiked with AuNP and ^{109}AgNP for a period of up to 3 weeks in two independent experiments. In this study we not only use real urban wastewater, but also environmentally relevant NP concentrations that are significantly lower than in comparable studies.

To investigate the fate of the NP within the WWTP, anaerobically digested sewage sludge and effluent from the spiked WWTP was collected over time. The WWTP effluent was used to investigate the uptake and accumulation of transformed compared to pristine NP. Additional uptake experiments with $^{109}Ag^{+}$ ions were performed (ionic control). The benthic freshwater amphipod *Hyalella azteca* was used for the uptake studies, as it is considered to be one of the most suitable invertebrates for NP bioaccumulation assessments and is currently being discussed as an alternative to the OECD fish test for bioaccumulation studies with NP (Kuehr et al., 2021a; OECD, 2024). Moreover, the uptake, elimination, and detoxification strategies for metals in *H. azteca* are well known (e.g. Poynton et al., 2019; Kuehr et al., 2021a; Borgmann et al., 1993; Kuehr et al., 2020a; Kuehr et al., 2021b).

AuNP were also incorporated in this study due to the low natural and anthropogenic background of Au and were used as a chemically conservative tracer, although we acknowledge, that also AuNP become reactive below a certain size (Avellan et al., 2020; Wielinski et al., 2021).

2. Material and methods

2.1. Nanoparticles

AuNP with a nominal diameter of 50 nm and a polyvinylpyrrolidone (PVP) coating (Econix - Gold Nanospheres) were purchased from nanoComposix.

Enriched ^{109}Ag (99.7 %) in metallic form was purchased from Isoflex USA. Isotopically enriched AgNP (^{109}AgNP) were synthesized from the metal using a modified protocol for seeded growth by Bastús et al. 2014 (Bastús et al., 2014). ^{109}AgNP were citrate-stabilized as from synthesis and not additionally coated. A detailed description of the ^{109}AgNP synthesis is provided in the supporting information (SI).

2.2. Characterization of the nanoparticles

The synthesized ^{109}AgNP were characterized by transmission electron microscopy (TEM), analytical centrifugation and ultraviolet–visible spectrophotometry (UV–Vis). The AuNP were characterized by TEM by the provider nanoComposix (Fig. S1). The hydrodynamic diameter and zeta potential (ζ-potential) of Au and ^{109}AgNP were determined by dynamic light scattering and electrophoretic light scattering (ELS) in MQ water, culture media (freshwater and brackish media) and WWTP control effluent, to assess the impact of the different exposure matrices on the NP characteristics. The metal content in the ^{109}AgNP stock, as well as in the ultra filtrate (to estimate the ^{109}Ag ionic fraction present) was measured by Inductively coupled plasma - mass spectrometry (ICP-MS). A description of the characterization methods and additional results not presented in the main document (e.g., analytical centrifugation, UV–vis extinction spectra and size distributions from DLS) can be found in the SI (Figs. S2–6).

2.3. Test organisms

All amphipods (*Hyalella azteca*) used in this study were obtained from cultures at the Swiss Federal Institute for Environmental Science and Technology (Eawag, Dübendorf, Switzerland) and the Norwegian Institute for Water Research (NIVA, Oslo, Norway), derived from the same strain (originally provided by Fraunhofer IME, Schmallenberg,

Germany). The culture procedure described in (Kuehr et al., 2020b) was adapted using 6 L glass aquaria filled with 5–6 L culture media (CM) (Borgmann, 1996) containing approximately 1′000 individuals.

2.4. Pilot wastewater treatment plant and spiking experiments

A pilot WWTP (Fig. 1) fed with municipal wastewater from the sewer network in Dübendorf, Switzerland after passing a primary clarifier was operated at Eawag (Dübendorf, Switzerland). The WWTP was operated with a wastewater flow of 16.8 L/h. A detailed description of the WWTP operation is provided in the SI. The given setup resulted in a sludge age of 22.3 days.

Gravimetric measurements of the total suspended solids (TSS) in activated and digested sludge were carried out after drying aliquots at 105 °C overnight (values presented in Table S1). Parameters including ammonium (NH_4^+), nitrite (NO_2^-) and nitrate (NO_3^-) concentrations and the chemical oxygen demand (COD) of the inflowing wastewater and the effluent were measured photometrically using cuvette kits (Hach Lange™) at least twice per week to monitor the performance of the WWTP. The mean reduction of COD was calculated based on the COD values of 0.45 μm filtered samples to exclude biological oxygen demand from microbes (Table S2).

Prior to the start of the first experiment, the effluent and digested sludge were collected and served as control samples for the subsequent experiments. A separate WWTP spiking experiment was conducted for each NP type, and the WWTP was completely cleaned after each experiment. After restarting the WWTP, an equilibration period of at least 2 weeks was allowed before the NP were spiked into the WWTP. During the experiments, Au or ^{109}Ag NP were spiked continuously into the nitrification unit (②, Fig. 1) and once per day, for 10 min during the mixing event, also into the thickener (④, Fig. 1). The spiking solutions were created by dilution of the initial NP stock dispersions with ultrapure water (MQ water). Table S3 provides detailed information about the concentrations and spiking rates of the respective spiking dispersions, which were freshly prepared every 72 h. Information about stability tests for the spiking dispersions are presented in the SI. Figs. S6 & S7 present the size distribution of hydrodynamic diameters before and after the spiking period. The spiking dispersions were stirred using a stirring plate and protected from light. Spiking was performed with peristaltic pumps (ISMATEC) and BPT tubing (Pharmed®). The flow rates and volumes of spiking dispersions required to achieve the target concentrations in the dried digested sludge were calculated treating the WWTP a continuously stirred tank reactor (Kaegi et al., 2011).

The spiking concentrations were calculated to result in environmentally realistic equilibrium concentrations in the sludge, but to be high enough to allow the quantitative detection of the respective isotopes against the background concentrations. The target concentrations in the dried digested sludge were 1 mg/kg for Au and 10 mg/kg for ^{109}Ag, dry weight (dw) and exceeded the respective limits of quantification by factors of about 10× to 20×, with the latter estimated from analyses of non-spiked samples. To achieve the desired concentration levels in the sludge within a reasonable time, higher flow rates (Table S3) of the NP stock suspensions were used during the first 72 h of the spiking (initial spiking) to load the sludge with a certain amount of NP. After the first 72 h spiking rates decreased to match the target concentration in the sludge (equilibrium spiking period). For the digested sludge, additional spiking with the NP into the thickener sludge mixed with primary sludge from the primary clarifier was performed once per day (④, Fig. 1). During the spiking experiment samples were collected from the denitrification unit (①, Fig. 1) and the effluent leaving the secondary clarifier (③; Fig. 1) every 2 h for the first 72 h of spiking and then at least once a day for up to 19 days to examine the NP or related isotope concentration by ICP-MS. Digested sludge was sampled once per day from the anaerobic digestor (⑤, Fig. 1). The digested sludge was collected, once the initial 72-h spiking phase was completed and stored at room temperature in 50 L plastic barrels. On the same days the effluent for the exposure experiments was collected during a 3 h period and stored in closed 25 L plastic canisters at 4 °C in the dark. The experiment continued until sufficient digested sludge was collected over the following days (up to 21 days). Details about the processing of the digested sludge are provided in the SI.

2.5. H. azteca uptake experiments with AuNP and ^{109}AgNP

The experiments were performed according to Kühr et al. (2018) (Kühr et al., 2018) with slight modifications (a schematic overview of the study can be found in Fig. S7). Adult animals between one and two months old were exposed for 7 days under static conditions with ad libitum feeding (milled fish food flakes, Tetramin®). Each treatment (Table 1) consisted of 5 replicates, each with 15 individuals in 500 mL exposure medium in a 600 mL glass beaker. The organisms were exposed to two concentrations of ^{109}AgNP-containing WWTP effluent (undiluted

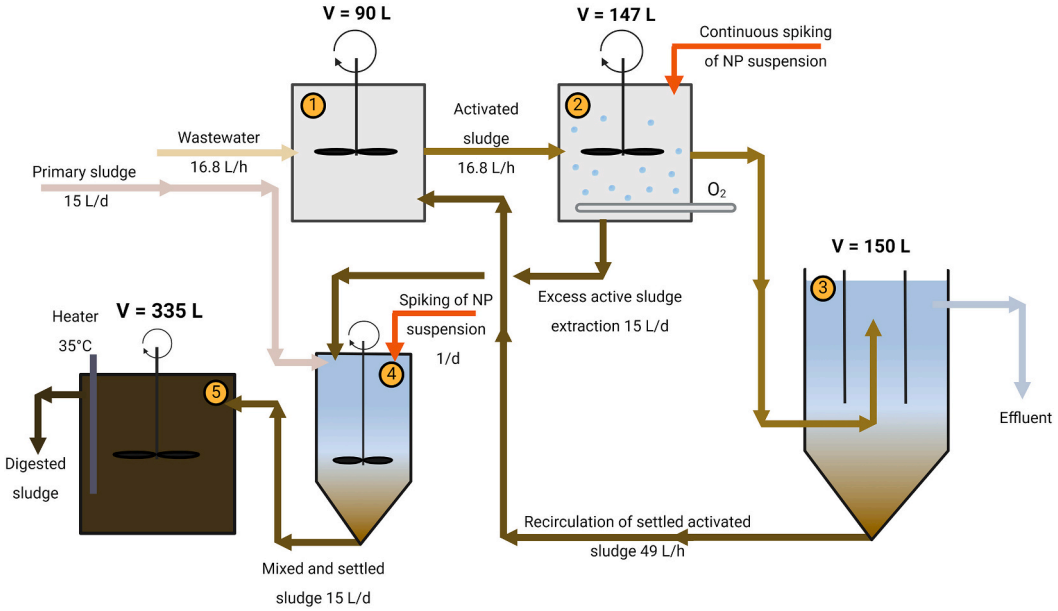

Fig. 1. Schematic overview of the pilot WWTP. ①: Denitrification unit; ②: Nitrification unit; ③: Secondary clarifier; ④: Thickener; ⑤: Anaerobic digestion unit.

and two times diluted with control effluent). Culture media and control effluent were included as controls. The concentration of Au in the effluent of the AuNP spiked-WWTP experiment was below detection limit. Thus, the AuNP exposure media were prepared from diluted (x1000, x2000) activated sludge collected during the AuNP spiking experiment. This strategy was chosen because the NP that will end up in the effluent of a WWTP will be bound to sludge flocs and are expected to be present at a concentration approximately 1′000 times lower compared to the activated sludge. To compare the bioavailability of pristine versus transformed NP, the organisms were also exposed to pristine ^{109}AgNP or AuNP spiked in culture media and control WWTP effluent. Additional experiments using $^{109}AgNO_3$ were carried out to allow a comparison of the nanoparticulate and ionic form of ^{109}Ag from exposure at comparable concentration levels.

As in some countries like Norway, WWTPs discharge the effluent into brackish water or marine systems (Tayeb et al., 2015; Al Aukidy and Verlicchi, 2017; Weigel et al., 2004), exposures under brackish water conditions were also performed. The survival rate of *H. azteca* was first determined in an initial test at different salinities (3 PSU – 15 PSU). Natural seawater (0.22 μm filtered, 35 PSU) collected from the outer Oslofjord was used to prepare the culture medium. The seawater was then diluted with MQ water-based culture medium to reach different salinity levels. Finally, the brackish exposures were performed at a 5 PSU salinity.

Exposures were carried out in the same way as for the WWTP effluents. Dried and ground digested sludge and the brackish culture medium (salinity 5 PSU) were used to prepare the respective brackish exposure media. Table 1 provides an overview of the treatments used in the study. The target concentrations were based on previous measurements of the effluent (e.g., 170 ng/L for ^{109}Ag) or activated sludge (e.g. 1.5 μg Au/L) from the spiked WWTP experiments.

At the start and end of the exposure, the pH and oxygen content of the media (mg/L and saturation in %) were determined (HQ30d flexi, HACH). At the end of the exposure, the animals were sampled, gently rinsed with MQ water, blotted dry, weighed, and euthanized by snap freezing in liquid nitrogen. The animals were then air-dried overnight at 40 °C in an incubator and stored at room temperature until further processing for analysis by ICP-MS.

2.6. Determination of total metal concentrations for WWTP matrices, synthesized NP stock suspensions, exposure media and test organisms

The determination of total Au for the WWTP matrices (activated sludge, effluent, digested sludge) during the WWTP experiment, as well as in the dried and milled digested sludge, and samples from the *H. azteca* freshwater exposure was carried out at Eawag (Dübendorf, Switzerland). Measurements of Ag in the WWTP matrices during the spiking experiment with ^{109}AgNP were also performed at Eawag for both ^{107}Ag and ^{109}Ag to allow monitoring of both isotope concentrations. The samples (triplicates) were digested using a microwave-assisted acid digestion system (MLS Germany). Further information on the digestion methods can be found in the SI. Measurements at Eawag were performed by ICP-MS using an Agilent 7700 ICP-Q-MS (Agilent Technologies) according to Wielinski et al. (2021) (Wielinski et al., 2021).

All other ICP-MS measurements for the isotope concentration determination and for Au in the test media and animals from the brackish treatments of the *H. azteca* uptake tests were performed at the Norwegian University of Life Science (NMBU, Ås, Norway). For the

Table 1
Overview of the AuNP and ^{109}AgNP treatments in the uptake tests with *H. azteca*.

Treatment	Exposure scenario
Au NP	
C	Culture medium control
EC	Control effluent (non-spiked WWTP, undiluted)
AuNP 1 & 2	Pristine AuNP in culture medium conc. 1 and 2
AuNP EC 1 & 2	Pristine AuNP spiked in control effluent conc. 1 and 2
AuNP S 1 & 2	Activated sludge from AuNP-spiked WWTP diluted in control effluent conc. 1 & 2
Au NP - brackish conditions (5 PSU)	
C	Brackish medium control
CS	Control Sludge: Digested sludge from non-spiked WWTP in brackish medium
AuNP 1 & 2	Pristine AuNP in brackish medium conc. 1 and 2
AuNP S 1 & 2	Digested sludge from AuNP-spiked WWTP experiment in brackish medium conc. 1 and 2
^{109}AgNP	
C	Culture medium control
EC	Control effluent (from non-spiked WWTP, undiluted)
CS EC	Control Sludge: Sludge from non-spiked WWTP suspended in control effluent
^{109}AgNP 1 & 2	Pristine ^{109}AgNP in culture medium conc. 1 and 2
^{109}AgNP EC 1 & 2	Pristine ^{109}AgNP spiked in control effluent conc. 1 and 2
^{109}AgNP EF 1 & 2	Effluent from ^{109}AgNP-spiked WWTP experiment conc. 1 and 2
^{109}AgNP - brackish conditions (5 PSU)	
C	Brackish culture medium control
CS	Control Sludge: Digested sludge from non-spiked WWTP suspended in brackish medium
^{109}AgNP 1 & 2	Pristine ^{109}AgNP in brackish culture medium conc. 1 and 2
^{109}AgNP S 1 & 2	Digested sludge from ^{109}AgNP-spiked WWTP experiment in brackish medium conc. 1 and 2
$^{109}Ag^+$	
$^{109}Ag^+$ 1 & 2	$^{109}AgNO_3$ in culture medium conc. 1 and 2
$^{109}Ag^+$ EC 1 & 2	$^{109}AgNO_3$ spiked in control effluent conc. 1 and 2
$^{109}Ag^+$ - brackish conditions (5 PSU)	
$^{109}Ag^+$ 1 & 2	$^{109}AgNO_3$ in brackish medium conc. 1 and 2

determination of Ag, the digested and diluted samples were measured four times using an Agilent 8900 instrument in oxygen reaction mode with ^{115}In as internal standard. The settings used for the determination of the Ag isotope concentration in the samples (Table S4), a schematic overview of interference removal during the determination of ^{107}Ag and ^{109}Ag concentrations, respectively (Figs. S10 & S11) and information on the calibration and isotope correction for the ^{109}Ag measurement are presented in the SI. The Au measurements were performed in oxygen reaction mode and Pt was used as internal standard at mass 195 (details of sample preparation are provided in the SI).

2.7. Data analysis

For the ICP-MS measurements, at least three analyses were performed for each sample and standard and the mean concentration was determined by the ICP-MS software (Agilent MassHunter V. 5.1).

The body burden ($C_{exp\ animal}$) as result of the uptake, determined for the respective metal/ isotope of each sample (in triplicates) from the exposed animals was corrected for the natural background (C_{nat}), as determined from analyses of animals from the culture media controls. The average corrected body burden ($C_{corr} = C_{exp\ animal} - C_{nat}$) of a treatment, was divided by the mean concentration (triplicates) of the respective metal/isotope in the exposure (C_{exp}) to obtain the accumulation factor ($AF = C_{corr}/C_{exp}$) (Kühr et al., 2018; Kuehr et al., 2020a).

Data and statistical analysis was performed using the software GraphPad Prism (version 9.4.1, San Diego, CA, USA). Data were assessed for normal distribution by a Shapiro-Wilk test. Significant differences between treatments were analyzed with one-way ANOVA followed by Tukey's multiple comparison test.

3. Results and discussion

3.1. Synthesis and characterization of ^{109}AgNP

3.1.1. TEM analysis

TEM images were analyzed with ImageJ/FIJI using a custom script (Sperling, n.d.) and revealed a few aggregates and other image artefacts that were excluded by minimum criteria for circularity (< 0.8) and size (d < 5–8 nm). A small number of rods were visible on the images and excluded from analysis (percentage of rods/ non-spherical particles was in a range of approx. 1–2 %). 1475 particles from 5 images were used to determine the mean diameter. ^{109}AgNP of near-spherical shape were synthesized with a mean diameter of 28.2 ± 6.8 nm (Fig. 2). These results were confirmed by analytical centrifugation using an optical detector operating at 405 nm wavelength (Fig. S1 & S2).

3.1.2. ICP-MS measurements

The ^{109}Ag concentration of the synthesized ^{109}AgNP suspension was 85 ± 1.1 mg/L. Analyses of the filtrate from the ultrafiltration showed that only 26 ng/L, or <0.01 %, of the ^{109}Ag in the stock suspension was present in dissolved form (≤ 10 kDa molecular weight cut-off) showing the suitability of the synthesis method. Details on the ultrafiltration method for ion separation are provided in the SI.

3.1.3. Dynamic light scattering (DLS) analysis

The hydrodynamic diameter of AuNP remained between 70 nm and 80 nm independent of the dispersion media (Table 2, Fig. S4). The size changes in the exposure media are <4 % compared to the mean value determined in MQ water. Considering the standard deviation, there is no clear difference in the hydrodynamic diameter of the AuNP between the freshwater and brackish media. According to the Derjaguin-Landau-Verey-Overbek (DLVO) theory, a high ionic strength (as in the brackish medium and the WWTP effluent) compresses the electrical double layer and reduces the surface charge of the particles, resulting in formation of agglomerates (Derjaguin et al., 1987; Quik et al., 2014; Lodeiro et al., 2016). The effect of the media on the ζ-potential is clearly visible: while the AuNP in MQ water have a negative ζ-potential of about

Table 2
Mean *Z*-average, Polydispersity Index (PDI) and ζ-potential values obtained for AuNP and ^{109}AgNP determined by DLS in different media at a concentration of 0.5 and 0.8 mg/L for AuNP and ^{109}AgNP, respectively. The values represent the mean of triplicates ($n = 3$) ± standard deviation (SD).

Matrix	mean Z-average [nm]	mean PDI	mean ζ-potential [mV]
AuNP			
MQ water	76.5 ± 0.8	0.087 ± 0.004	−19.3 ± 1.0
Culture medium	73.8 ± 0.4	0.076 ± 0.012	−4.4 ± 0.4
Brackish medium	74.2 ± 0.8	0.085 ± 0.017	−9.2 ± 1.3
CTRL effluent	78.1 ± 0.3	0.062 ± 0.004	−3.4 ± 0.4
^{109}AgNP			
MQ water	22.0 ± 0.2	0.542 ± 0.00	−48.6 ± 1.5
Culture medium	51.4 ± 0.7	0.314 ± 0.031	−17.9 ± 0.4
Brackish medium	320.6 ± 29.3	0.387 ± 0.017	−18.2 ± 0.5
CTRL effluent	280.7 ± 14.6	0.285 ± 0.010	−20.1 ± 0.8

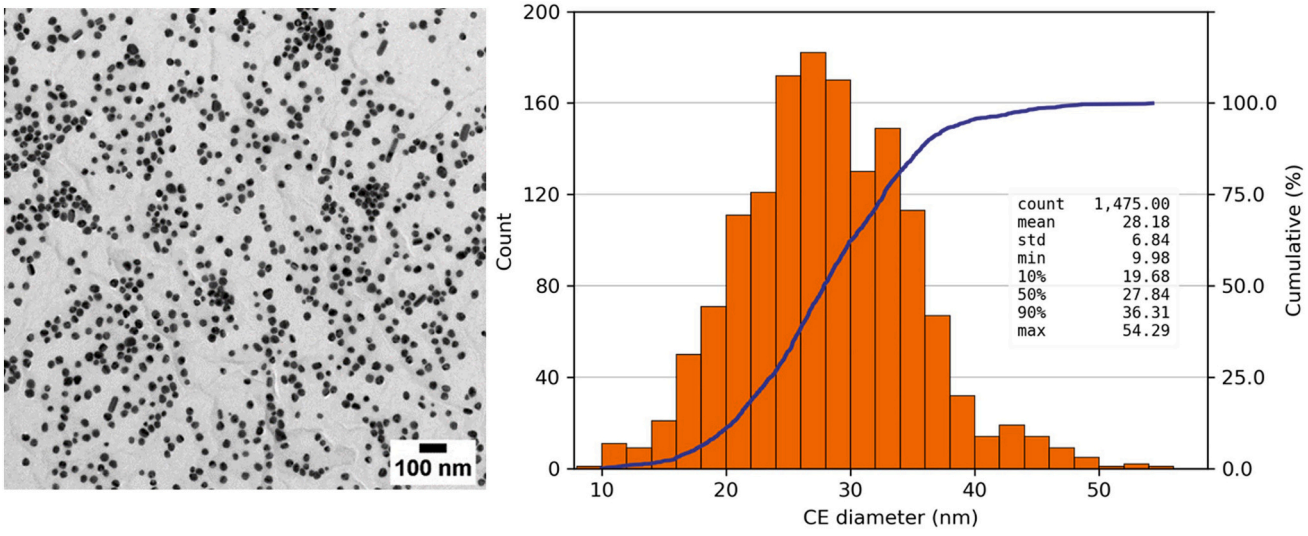

Fig. 2. Left: A representative TEM image of the synthesized ^{109}AgNP used to determine the mean size of the particles. Right: Histogram build from five TEM images including the examination of 1475 particles presenting the size distribution: Given values like mean, minimum (min) and maximum (max) sizes are in nm.

−19 mV, this is much less pronounced in all other media and is only about −3.4 mV in the control effluent which should result in an increase in the particle diameter due to aggregation. García- Negrete et al. (2013) and Sikder et al. (2018) described the aggregation of AuNP in seawater and showed that aggregate formation is strongly correlated with the AuNP concentration (García-Negrete et al., 2013; Sikder et al., 2018).

As our analyses were conducted at a AuNP concentration several times lower (0.5 mg/L) than the 30 mg/L used by García- Negrete et al. (2013), at shorter incubation periods and lower salinity (5 PSU versus 35 PSU of seawater (Millero et al., 2008)), no strong aggregation was observed in this study. The presence of the AuNP in a narrow size distribution (only non-aggregated AuNP) is also indicated by the values of the polydispersity Index (PDI as square of the light scattering polydispersity, Table 2) (Malvern Panalytical, 2017). Furthermore, it has been shown that natural organic matter (NOM) such as humic and fulvic acids, which are expected to be present in wastewater and seawater, can enhance or generate the electrostatic repulsive forces and steric effects by formation of a NOM corona. This finally leads to a reduced tendency for (homo)aggregation (Tan et al., 2023). The different exposure media had a stronger influence on the hydrodynamic diameter of ^{109}AgNP (Table 2, Fig. S5). From about 22 nm in MQ water, the hydrodynamic diameter of the particles more than doubled in the culture medium (51 nm). In the brackish culture medium and in the control effluent the diameters were >10 times larger than in MQ water, indicating the formation of aggregates, as expected based on the DLVO theory and in agreement with previous observations (e.g., (Stuart et al., 2013)). A decrease in the ^{109}AgNP ζ–potential from −49 mV in MQ water to −18 and − 20 mV in culture medium or brackish medium (5 PSU) and CTRL effluent, respectively (Table 2) was observed which is in agreement with the DLVO theory.

3.2. Wastewater treatment plant spiking experiments

3.2.1. WWTP stability and performance

The stability and performance of the wastewater treatment plant was evaluated by regularly monitoring the COD, the NH_4^+, NO_2^-, NO_3^- concentrations in the influent/wastewater and effluent, and the TSS content in the activated and digested sludge (Sundara Kumar et al., 2010) during both the equilibration and spiking phases of the experiments.

The measured values of <0.2 mg/L NH_4^+ and NO_2^- and 20.4 mg/L NO_3^-in the effluent obtained during the test period (Table S2), show that the oxidation of NH_4^+ in the WWTP was complete.

On average, the WWTP achieved a COD reduction in the wastewater of approximately 86 % compared to the average COD values in the influent and effluent of the WWTP (Table S2). The treatment performance of the system was not affected by the spiking experiments with AuNP or ^{109}AgNP (Table S1).

3.2.2. Spiking of AuNP

During the first 3 days, the Au concentration in activated and digested sludge increased as expected (Fig. 3). From the initial concentrations of around 1 μg Au/L in the liquid activated sludge (Fig. 3 A) and around 3 μg/L in the liquid digested sludge (Fig. 3 B), the Au concentrations increased to 1.6 μg/L and 9.5 μg/kg, respectively, during the 72 h initial spiking phase (Fig. 3 B).

During the subsequent equilibrium spiking period, the Au concentration in the activated sludge remained relatively constant at around 1 to 1.5 μg/L (Fig. 3 A). A stable concentration of approximately 14 μg/kg was measured in the digested sludge with a delay of 24 h after the end of the initial spiking period (Fig. 3 B), as the AuNP from the spiking of the thickener arrives in the digested sludge only after the thickened activated sludge has been transferred to the digester.

A concentration of 2.57 ± 0.03 mg Au/kg (dw) was measured in the final dried digested sludge. If the natural/anthropogenic background of 0.57 mg Au/kg (measured in the dried control digested sludge) is subtracted, the spiking of the WWTP resulted in an additional Au concentration of 2 mg/kg in the dried digested sludge. This is a factor of 2 higher than the target concentration of 1 mg/kg (dw) and this difference might be explained by the TSS content of the liquid digested sludge (see SI).

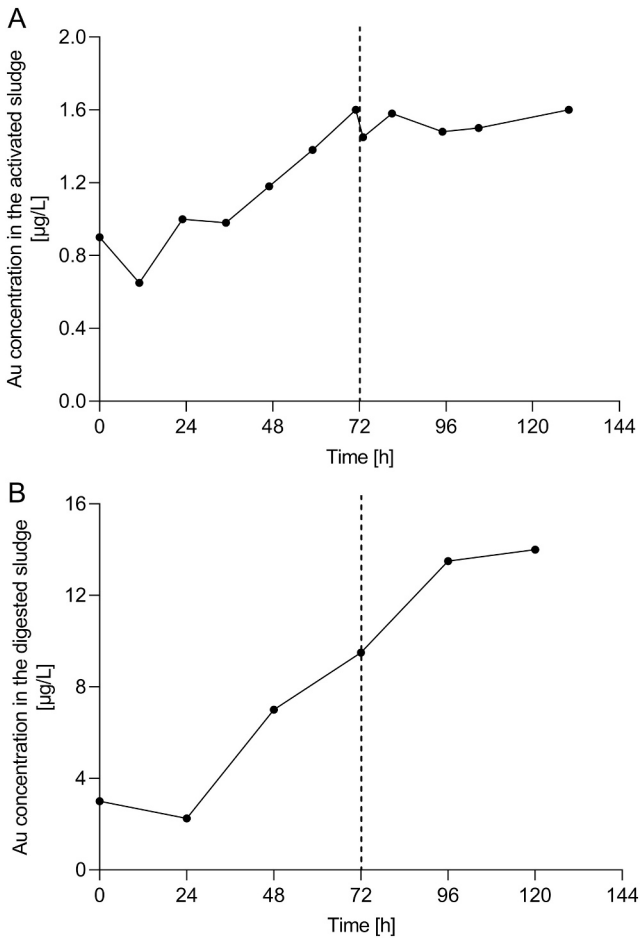

Fig. 3. Au concentration in μg/L (n = 1) measured in samples from (A) the liquid activated sludge (nitrification unit) taken during the course of the AuNP spiking experiment and (B) the digested sludge (before drying). The dashed lines represent the end of the 72 h initial spiking and start of the equilibrium spiking period.

The spiking calculations were based on TSS measurements of fresh digested sludge from the WWTP "ARA Neugut-Dübendorf" (Switzerland) which was used to inoculate the anaerobic digester. However, as reported in the SI, the TSS content of the digested sludge decreased during the course of the experiments, which may have resulted in a higher load of AuNP per g of TSS in the digested sludge. Nonetheless, the measured AuNP concentration is still up to 2500 times lower than that used in comparable studies (e.g. (Hund-Rinke et al., 2021; Schlich et al., 2021)). The Au concentration in the effluent was below the detection limit of 0.1 ng/L throughout the WWTP experiment. This suggests that all Au was bound to the sludge particles and that sludge flocs were not significantly released via the effluent at the time of effluent sampling.

3.2.3. Spiking of ^{109}AgNP

The ^{109}Ag concentrations in the activated sludge, digested sludge and effluent increased as expected during the initial 72-hour spiking period (Fig. 4). During the initial spiking phase, the ^{109}Ag concentrations in the activated sludge increased from initially 4.8 μg/L to 25–30 μg/L (Fig. 4 A). The relative concentrations of the two Ag isotopes are initially in the natural ratio but as the spiking process progresses the

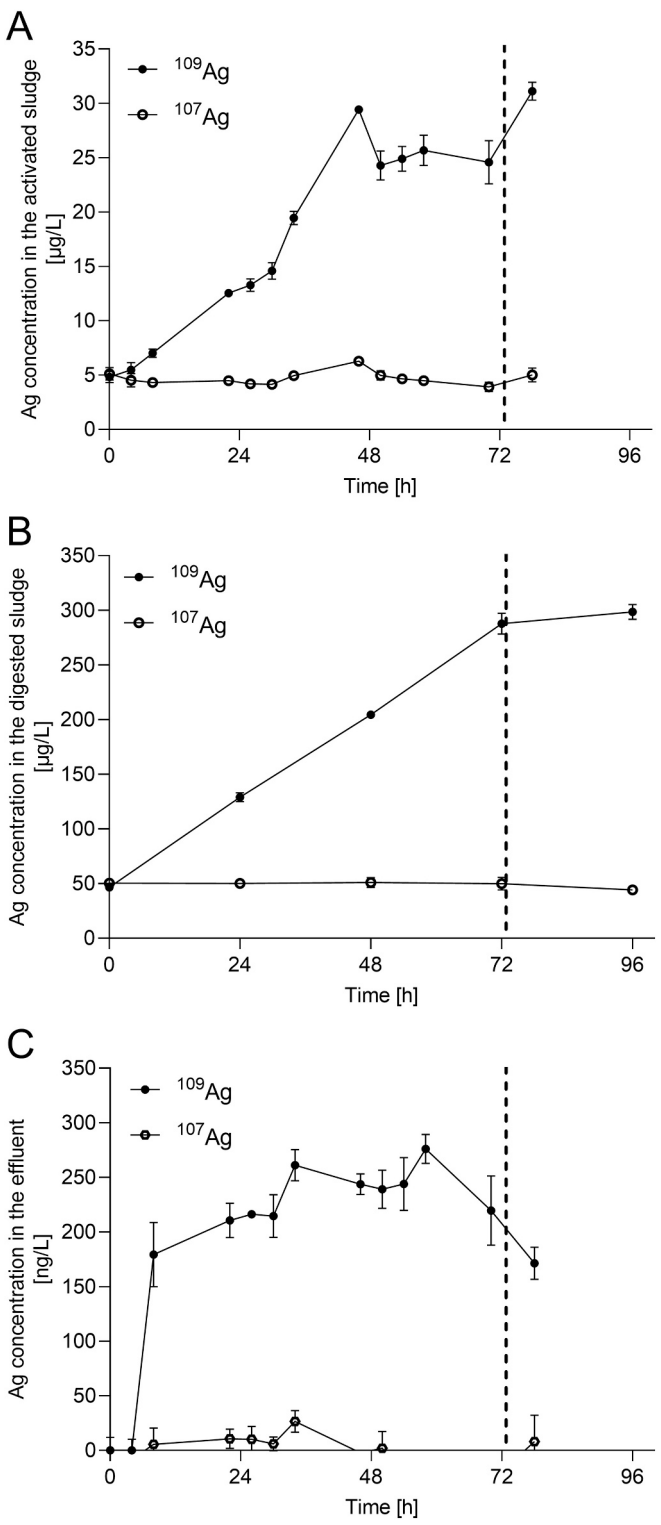

Fig. 4. Ag concentration in µg/L ± SD (n = 3) measured in samples collected from the WWTP during the ^{109}AgNP spiking experiment. The dashed lines represent the end of the 72 hlasting initial spiking and start of the equilibrium spiking period. Ag concentration in the (A) activated sludge (nitrification unit) in µg Ag/L ± SD (n = 3), (B) digested sludge (before drying) in µg Ag/L ± SD (n = 3) and (C) effluent in ng Ag/L ± SD (n = 3).

^{109}Ag concentration increases while the ^{107}Ag concentration remains at a stable and low level (5 µg/L). After 4 h, the relative abundances of the two Ag isotopes were clearly different from the natural ratio. The same behavior of increasing ^{109}Ag and corresponding stable ^{107}Ag concentrations was also seen for the digested sludge (Fig. 4 B). At the end of the experiment the final concentration of ^{109}Ag was around 300 µg/L in the liquid digested sludge and 19.9 ± 0.1 mg/kg in the dried digested sludge. Similarly to the AuNP spiking experiment, the measured concentration in the digested sludge was about two times higher than the target concentration of 10 mg ^{109}Ag /kg, and this can again be explained by differences in the TSS content of the digested sludge. Comparing the data with the measured particulate Ag concentrations of 3–14 mg/kg (dw) determined in British WWTPs between 2014 and 2018, the concentration is still within an environmentally realistic range (Johnson et al., 2014). This is particularly valid given the increase in the production and use of AgNP in recent years (Inshakova and Inshakov, 2017; Hou et al., 2017).

The ^{109}Ag concentration in the effluent increased from an initial concentration of about 4 ng/L to about 200 ng/L within the first 12 h. After 36 h (Fig. 4 C), it fluctuated between 220 and 276 ng/L and dropped down to 170 ng/L within the first hours of the equilibrium spiking phase. The ^{109}Ag concentrations of the effluent collected for the uptake test and the control effluent were 152.3 ± 5.7 ng/L and below the detection limit (< 6.8 ng/L), respectively. According to previous studies, the modeled Ag concentrations in WWTP effluents were about 40 ng/L (Gottschalk et al., 2009) while analyses of river water collected near a WWTP showed Ag levels of about 70 ng/L for nanoparticulate silver alone (Wimmer et al., 2019). It should be noted that whilst the samples were taken close to the WWTP discharge point, dilution of the effluent by the river water had already occurred at the point of collection. Thus, ^{109}Ag concentration in the effluent collected during the ^{109}Ag WWTP spiking experiment is at an environmentally relevant level.

3.3. *H. azteca uptake studies*

At the start and end of the uptake test, the pH, oxygen concentration and saturation were quantified to ascertain that the exposure did not encompass conditions that could have a deleterious impact on the animals and consequently influence their physiology or behavior. The pH values observed across the treatments of the tests ranged between 7.5 (^{109}AgNP EF 1) and 8.3 (C- 5PSU, Au study). The oxygen concentration and saturation levels were in a range of 7.94 mg/L (92.4 %; AuNP1) and 8.24 mg/L (97.3 %; ^{109}AgNP EF 2). The data indicates that the animals were not affected by these parameters. This is also reflected by the low mortality rates (8–11 %) observed in all treatments and controls.

3.3.1. *AuNP uptake – freshwater conditions*

Approximately 10 ng/L of Au were measured in the media of the control WWTP effluent treatment (EC). The tissue concentrations of the respective animals after 7 days of exposure were, like the natural background (determined from the “C” treatment animals), below LOD and therefore no AF was calculated.

Pristine AuNP in freshwater media (AuNP 1 & 2) at concentrations of 35 ± 5 and 64 ± 3 ng Au/L resulted in AF values of 61 and 54 (Fig. 5 A), respectively. These results indicate a lower uptake and accumulation than previously observed in a comparable exposure of *H. azteca* to AuNP by Kuehr et al. (2020b) in the same media, where AF values of 166 to 424 were determined after 7 days of exposure to 700 and 85 ng Au/L, respectively (Kuehr et al., 2020b).

However, the AuNP used in our study have a more negative ζ–potential (Kuehr et al., 2021b; Kuehr et al., 2020b). For AuNP, clathrin-mediated endocytosis is considered as the main route of AuNP uptake into tissues (Shukla et al., 2005; Chithrani and Chan, 2007; Nativo et al., 2008). Increasing negative ζ–potentials significantly reduce the rate of endocytosis, and this may explain the reduced uptake and accumulation of Au in the current experiment (Harush-Frenkel

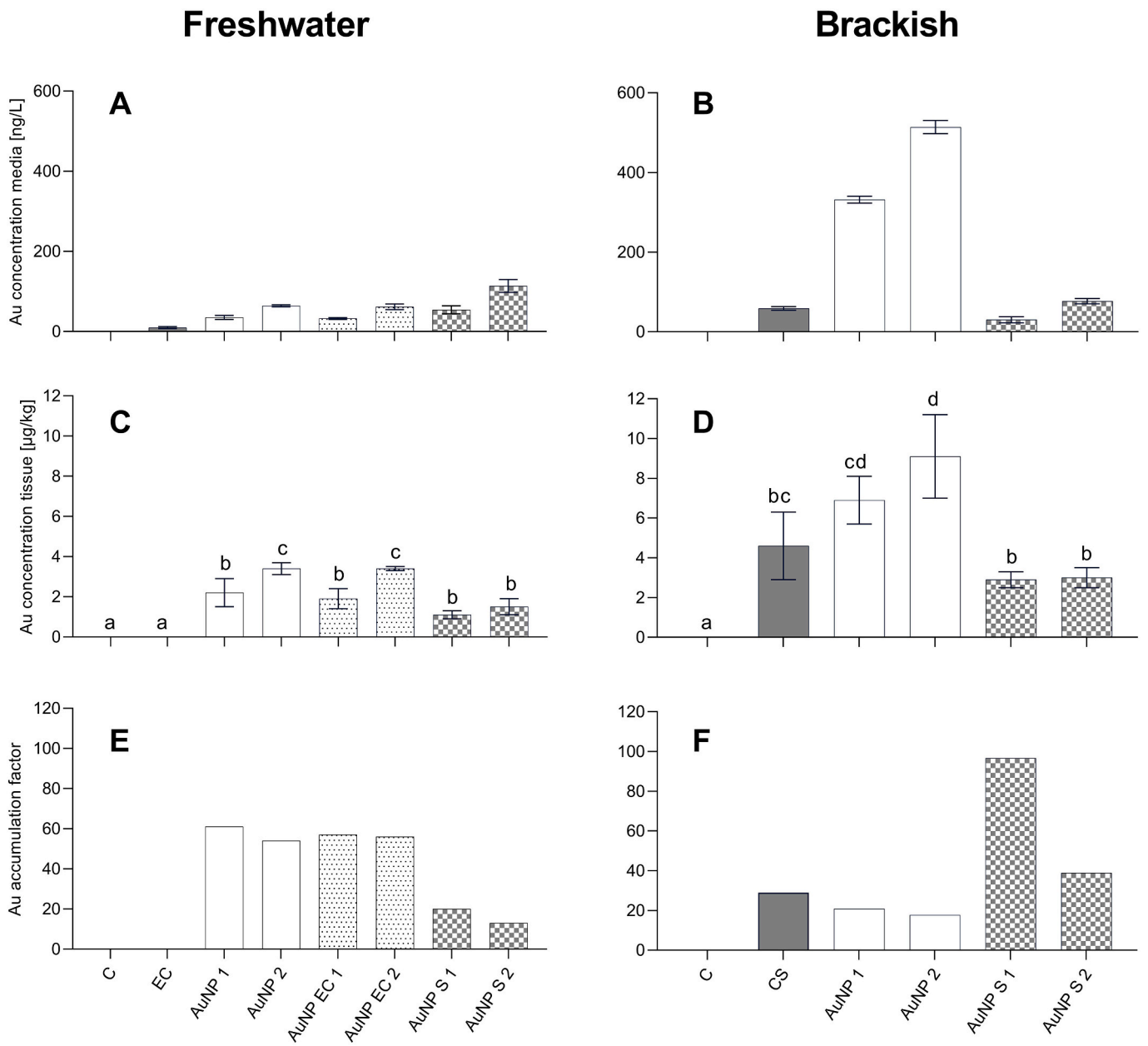

Fig. 5. Overview of results obtained with the 7-day *H. azteca* uptake test with AuNP in freshwater (A, C, E) and brackish (B, D, F) exposures. Au concentration in exposure media (A, B) [ng/L] ± SD, $n = 3$; Au concentration in *H. azteca* tissue (C, D) [µg/kg] ± SD, n = 3 (20 animals per replicate); Au accumulation factors (D, F). There was no measurable Au in the culture medium (A, B) and respective animals (C, D). Therefore, no AF values were calculated for these treatments. Different lowercase letters denote significant differences among treatments.

et al., 2007). This is also supported by the results of Cho et al. (2009), who found that the uptake of AuNP with a positive ζ–potential by breast cancer cells was 5–10 times higher than that of negatively charged AuNP, with neutral AuNP also being taken up more rapidly (Cho et al., 2009).

Exposure of *H. azteca* to media containing AuNP from the activated sludge of the WWTP (treatments AuNP S 1 (54 ng Au/L) & 2 (114 ng Au/L)) resulted in AF values of 20 and 13 (Fig. 5 E), respectively. Surprisingly, these values are lower than those obtained for pristine AuNP (AuNP 1 & 2, Fig. 5 E) despite the similar measured Au exposure levels. Due to the inert nature of Au, no chemical transformation, which could be responsible for the altered uptake, is expected. However, it has been shown that AuNP acquire a corona of NOM when added to wastewater media. This can occur either by adsorption onto an existing coating, such as PVP (overcoating), or directly onto the particle surface by replacing the existing coating (displacement) (Surette et al., 2019; Surette et al., 2021).

Such corona formation affects the physical properties, and thus the aggregation and sedimentation behavior of the AuNP but also the uptake and potential accumulation due to the altered particle size and surface properties (Ding et al., 2018). The altered surface charge also affects the adhesion of NPs to biological membranes, which can lead to reduced adhesion-induced uptake, as described by Cheng et al. in 2015 (Cheng et al., 2015).

The DLS analyses, however, provided no evidence for the formation of large AuNP aggregates (Table 2). Exposure to AuNP spiked to control effluent (AuNP EC1 & 2, Fig. 5 E) led to similar AF values compared to pristine AuNP.

Surette et al. (2019) showed that, depending on the NOM composition, different coronas with different properties are formed that can

influence the NP behavior in different ways (Surette et al., 2019). It has been previously shown that exposure of *H. azteca* to polystyrene NP via the protein- and polysaccharide-rich pseudo-feces of mussels led to significantly higher AF values due to the presence of attached macromolecules, than the exposure to the pristine counterparts (Kuehr et al., 2021b).

The microbial composition of a matrix and its aquatic chemistry have a significant influence on the NOM composition (Sheng et al., 2010; Dignac et al., 1998; Zeng et al., 2016). For COOH-functionalized AuNP, it was shown that different aggregates were formed in the distinct matrices of the nitrification and denitrification stages of a wastewater treatment plant. That was explained by variations in the extracellular polymeric substances (released by microbes) that were forming the corona (Surette et al., 2019).

Together, these findings help to explain the significantly different AF values determined for the pristine AuNP and the AuNP S 1 & 2 treatments. The AuNP from the AuNP S 1 & 2 treatments likely had a different corona compared to the pristine AuNP spiked in the control effluent (C AuNP EC 1 & 2), as they originated from the activated sludge of the nitrification unit. However, this could not be confirmed via DLS, as DLS measurements could only be performed with AuNP spiked into the filtered (0.45 μm) control effluent but not with the activated sludge containing AuNP due to the high load of TSS.

3.3.2. *AuNP uptake – brackish conditions*

The impact of the high ionic strength of the brackish media on the uptake of the AuNP was investigated.

For pristine AuNP in brackish media AF values of 21 and 18 were obtained (AuNP 1 & AuNP 2, Fig. 5 F). While the aggregation of AuNP in seawater was previously described, it has also been suggested that surface coatings such as PVP could counteract their aggregation behavior (García-Negrete et al., 2013; Stakenborg et al., 2008). As discussed above for the freshwater conditions, the uptake of AuNP can alternatively be altered by the formation of a corona. Dissolved NOM, such as

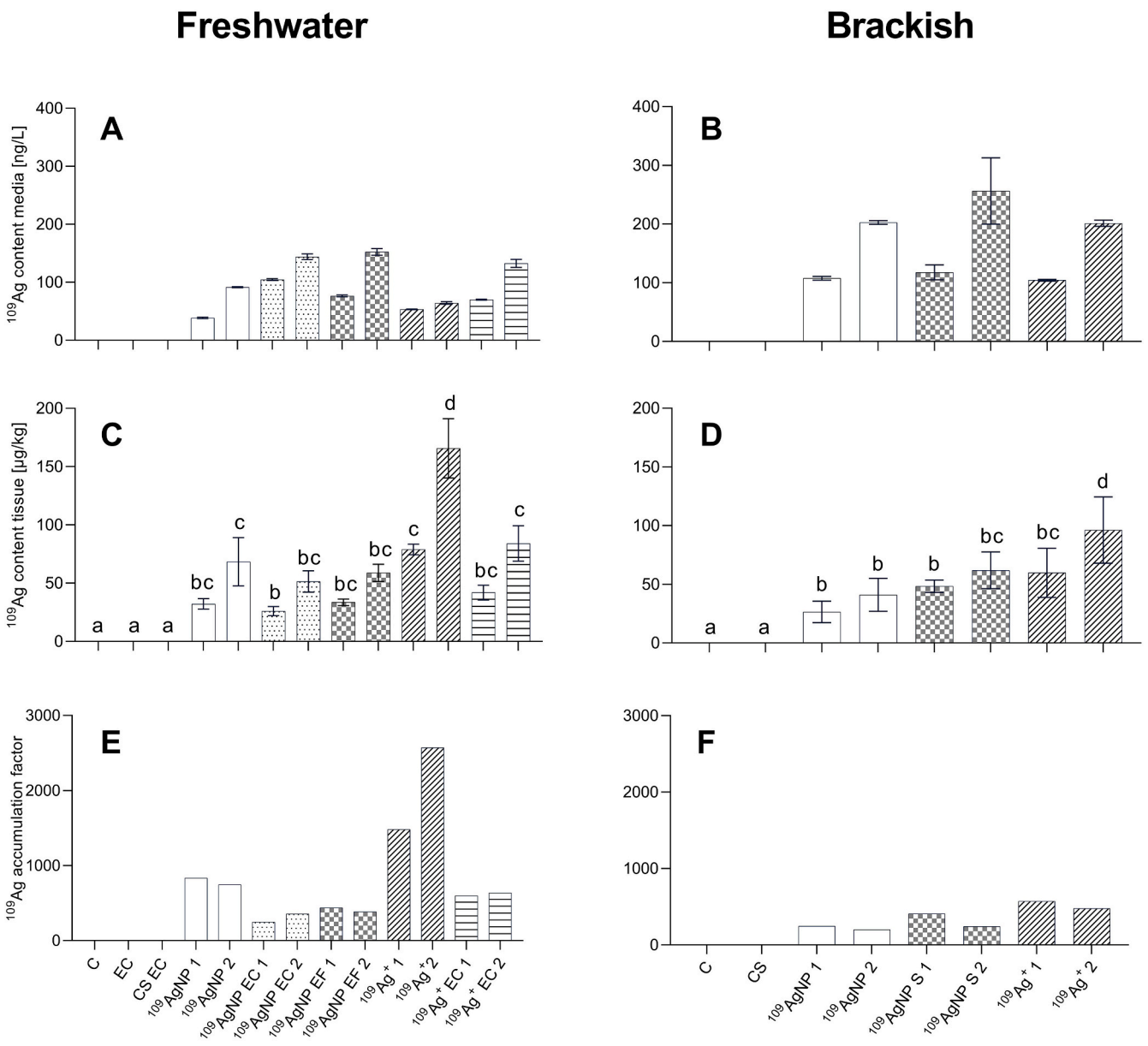

Fig. 6. Overview of results obtained with the 7 day *H. azteca* uptake test with ^{109}AgNP and ^{109}Ag ions in freshwater (A, C, E) and brackish (B, D, F) exposures. ^{109}Ag concentration in exposure media (A, B) [ng/L] ± SD, $n = 3$;.^{109}Ag content in *H. azteca* tissue (C, D) [μg/kg] ± SD, n = 3 (15 animals per replicate);^{109}Ag accumulation factors (E, F). The concentration of ^{109}Ag in all control media (C, EC; CS EC and CS; A, B) and respective animals (C, D) were below the detection limit. Therefore, no AF values were calculated for these treatments. Different lowercase letters denote significant differences among treatments.

extracellular polymeric substances from microbes and algae, that were not removed by seawater filtration (0.22 μm) could have led to corona formation, explaining the reduced uptake of AuNP in all brackish treatments.

The presence of an Au background in the digested control sludge resulted in an Au exposure concentration of about 60 ng/L and an AF of 29 for the non-spiked control sludge treatment (CS, Fig. 5 B & D). No statement can be made about the characteristics of the Au already present in the untreated wastewater and hence in the control sludge. The Au uptake routes, or incorporation processes are therefore unconstrained, but a simple explanation would be uptake of Au or AuNP by the amphipods through consumption of the digested sludge. The use of sewage sludge as a food source by *H. azteca* was previously reported and sludge was visible in the digestive tract of organisms from this and previous experiments (Kühr et al., 2018; Kuehr et al., 2020a). A simple uptake process by ingestion of digested sludge may also explain the measured body burden of *H. azteca* exposed to digested sludge from the spiked WWTP in brackish media (AuNP S 1 & 2; Fig. 5 D). To address the bioavailability of Au (and thus the incorporation of Au into the tissue of the animals), the kinetics of the body burden during an elimination phase should be investigated in future studies.

3.3.3. ^{109}AgNP uptake – freshwater conditions

A particular advantage of the isotope labeling approach was that we were able to specifically study the fate and uptake of ^{109}Ag from the ^{109}AgNP that were spiked into the WWTP and subsequently used for the uptake experiments. Exposure to pristine ^{109}AgNP at 40 and 90 ng/L (Fig. 6 A) led to similar AF values of 830 and 750 for ^{109}Ag (Fig. 6 E).

Exposure to ^{109}AgNP-containing WWTP effluent (^{109}AgNP EF 1 & 2) or ^{109}AgNP spiked in control effluent (^{109}AgNP EC 1 & 2; Fig. 6 A) led to 2 times lower AF compared to the exposure to pristine ^{109}AgNP (250–440 vs 750–830; Fig. 6 E). Particle aggregation induced by the higher ionic strength of the effluent (^{109}AgNP size of 280.7 ± 14.6 nm in effluent according to DLS measurement, Table 2) and corona formation and sulfidation due to the presence of NOM and sulfides in the wastewater matrices, respectively can cause a reduction in Ag^+ release and reduced uptake (Kaegi et al., 2013). The highest AF were observed upon exposure to $^{109}AgNO_3$ in culture media at similar concentrations as for the ^{109}Ag measured in the effluent collected from the ^{109}AgNP spiked WWTP. The AF values obtained for $^{109}Ag^+$ with 50 ng/L ($^{109}Ag^+$ 1: 1480) and 60 ng/L ($^{109}Ag^+$ 2: 2540, Fig. 6 E) were 2 to 3 times higher than those determined for ^{109}AgNP spiked into culture media with 40 ng/L (^{109}AgNP 1: 570 & 2: 480, Fig. 6 E). The higher AF values for $^{109}Ag^+$ compared to ^{109}AgNP are in agreement with previously reported results from *H. azteca* bioconcentration tests that used $AgNO_3$ and AgNP (prepared from natural Ag) and the same media (Kuehr et al., 2020b).

The uptake of dissolved Ag in the form of Ag^+ ions or dissolved Ag complexes is considered to be the major uptake pathway for Ag during exposures of *H. azteca* and other aquatic species to AgNP (Kuehr et al., 2020a; Kuehr, 2021). However, the particles themselves are potentially also available via the mechanisms discussed above for the AuNP (e.g. dietary uptake and protein transport). However, ions are also released by oxidation of Ag^0 from the AgNP in the aqueous environment, potentially increasing the metal uptake (Wimmer et al., 2020).

Ag^+ can then be taken up by most species via Na^+ channels and Cu transporters and this uptake routes seem to be more efficient and faster than those for particles (Wang and Wang, 2014; Lee et al., 2002; Bertinato et al., 2010).

Exposure of *H. azteca* to $^{109}AgNO_3$ spiked into the control effluent ($^{109}Ag^+$ EC 1 & 2) resulted in AF values that were (i) 3–4 times lower (at 600 and 640) compared to exposures where $^{109}AgNO_3$ was added to the culture media ($^{109}Ag^+$ 1 & 2; AF of 1480 & 2540; Fig. 6 E) and (ii) comparable to the AF values obtained with the pristine ^{109}AgNP in culture media (^{109}AgNP 1 & 2; AF of 840 and 750; Fig. 6 E). Several processes may be responsible for the reduced uptake of the ionic ^{109}Ag during the exposure via the control effluent. On one hand, this may reflect that ^{109}Ag ions can bind to the organic matter present in the effluent and they can also precipitate as Ag_2S resulting in strongly reduced uptake of the Ag (Kühr et al., 2018; Georgantzopoulou et al., 2020; Georgantzopoulou et al., 2018; Kuehr et al., 2021b; Kampe et al., 2018; Zeumer et al., 2020b). On the other hand, it may be related to the formation of secondary AgNP, that may be produced following reduction of Ag^+ ions to Ag^0 by humic acids (Ding et al., 2019).

Surprisingly, the pristine ^{109}AgNP that were spiked into the control effluent (^{109}AgNP EC 1 & 2) had similar or slightly lower AF values (of 250 and 360, Fig. 6 E) compared to those observed for ^{109}AgNP that had passed through the WWTP (^{109}AgNP EF 1 & 2, AF values of 440 and 390), for exposures conducted at comparable concentrations (Fig. 6 E). In studies using artificial wastewater, Ag from AgNP that passed through a WWTP was taken up less than Ag from AgNP that were only spiked into the WWTP effluent shortly prior to the exposure (Kühr et al., 2018; Zeumer et al., 2020b). The composition of the effluent and the microbiome within the WWTPs, and thus the different forms of macromolecular coronas that are formed, are most likely responsible for these observations. However, also differences in temperature, pH or Eh values cannot be excluded as the cause of different transformations and their extend. This indicates that the use of real or artificial wastewater in exposure experiments can affect the extent of AgNP transformations and resulting changes in the uptake of NP and potential ions released from them.

3.3.4. ^{109}AgNP uptake – brackish conditions

For the brackish control media (C and CS) (Fig. 6 B) and in the corresponding organisms (Fig. 6 D) the ^{109}Ag concentrations were below the detection limit.

Brackish media appear to eliminate the differences in the uptake of pristine and transformed ^{109}AgNP. In detail, a lower ^{109}Ag uptake compared to the freshwater media, resulting in AF values ranging from 200 to 410, was observed for all ^{109}AgNP treatments in brackish media (Fig. 6 F). The most pronounced reduction in ^{109}Ag uptake was observed for exposures with $^{109}AgNO_3$ in the brackish as opposed to the freshwater treatments ($^{109}Ag^+$ 1 &2), with resulting AF values of 570 and 480 for the brackish treatments $^{109}Ag^+$ 1 & 2 (with exposure concentrations of 100 and 200 ng ^{109}Ag/L, Fig. 6 B). This observation is in agreement with previously obtained results for *H. azteca* exposed to $AgNO_3$ in the presence of digested sludge (Kuehr et al., 2020a).

Thermodynamic calculations suggest that whilst Ag species such as AgCl, Ag_2S and Ag^0 are dominant in freshwater environments, $AgCl_x^{(x-1)}$ is the main Ag form in seawater systems due to the high concentration of Cl^- ions (Levard et al., 2012). The latter complexes are well soluble and therefore more bioavailable compared to Ag_2S (Levard et al., 2012). The sparingly soluble AgCl will only be present at low salinities but even at a salinity of 5 PSU (as in our brackish treatments), the Cl^- concentration is 2.8 g Cl^-/L, thus resulting in a strong excess of Cl^- over Ag. This means that media with a salinity of 5 PSU favor the formation of $AgClx^{(x-1)}$ complexes. Thus, in the 5 PSU exposure scenario, the dissolution of AgNP may be the dominant fate of AgNP compared to the formation of aggregates. This is supported by the results of Toncelli et al. (2017), who found that the presence of NOM or the sulfidation of AgNP does not prevent the dissolution of AgNP in seawater, with about 76 % of Ag_2SNP dissolved after 3 h and about 91–99 % after 72 h (Toncelli et al., 2017).

However, the formation of $AgCl_x^{(x-1)}$ complexes in brackish media still reduces the uptake of Ag compared to freshwater conditions. Negatively charged Ag species such as $AgCl_x^{(x-1)}$ complexes are difficult to be taken up by Na^+ channels or high-affinity Cu transporters, which favor positively charged Ag species (Lee et al., 2002; Bertinato et al., 2010; Evans et al., 2005). Similar arguments hold true for uptake mechanisms working for neutral Ag species (Bury and Hogstrand, 2002; Hogstrand, 2003). At even higher Cl^- levels, for example in seawater with a salinity of around 35 PSU, the formation of negatively charged $AgCl_x^{(x-1)}$ complexes would be even more pronounced, most likely resulting in an even lower uptake than observed in this study.

3.4. Conclusion and environmental significance

Ionic silver Ag^+, is one of the most toxic metals to aquatic biota. It has therefore found widespread use as a fungicide and in numerous antimicrobial formulations including in textiles. The nanoparticulate form of Ag makes the application more efficient because it allows slow release of Ag^+. Most of the AgNP utilized in different products end up in WWTP sludge, as this and previous related studies have shown. Studies on the fate and toxicity to aquatic biota of WWTP-based AgNP at environmentally relevant Ag concentrations are challenging because the effluent already contains relatively high Ag concentrations from different sources. Thus, the previous studies have resorted to using high concentration levels of AgNP in combination with synthetic wastewater. In this study, we overcame this challenge by using isotopically enriched ^{109}AgNP. The use of enriched ^{109}AgNP allowed us to use environmentally relevant AgNP concentrations and real (rather than synthetic) wastewater in our spiking and exposure experiments. Both significantly increased the proximity to real conditions and allowed the subsequent exposure of the benthic amphipod *H. azteca* to more realistic conditions. The fate of AuNP and AgNP were studied at environmentally relevant concentrations of 30 to 500 ng Au/L and 39 to 260 ng Ag/L in comprehensive investigations, which extended from WWTP processes to the accumulation in amphipods.

By using AuNP as a chemically almost inert NP in our exposure experiments, we showed that other transformation processes (e.g. formation of a bio- or eco-corona), might be responsible for the reduced NP uptake (in addition to chemical transformation).

Transformation processes induced by exposing environmentally relevant concentrations of NP in brackish media appear to reduce the uptake of Au and Ag to an even greater extent compared to wastewater matrices. Even brief contact of ^{109}AgNP with the WWTP effluent (simulated by spiking ^{109}AgNP into control effluent matrices) resulted in strongly decreased AF values (250–350) compared to the AF values obtained for the pristine material (750–840). Contact with the brackish control medium reduced the AF values of ^{109}Ag, but also Au by around three times.

Based on the obtained data it is still unclear, however, whether the body burdens measured for ^{109}Ag, result from the uptake of NP or ions. The same applies to the question of whether the measured concentrations of ^{109}Ag and Au in the exposed amphipods result from the uptake of material that is bioavailable and incorporated into tissues or simply ingested material (e.g. present in the gut) that can be easily and fast excreted with the feces.

These questions can be addressed by carrying out kinetic exposure studies that include a depuration phase combined with measuring AgNP (rather than Ag^+) concentration using single particle ICP-MS. Our work highlights the importance of incorporating environmental relevance in studies that investigate the fate, bioavailability and toxicity of NM, by taking into account both NP transformations and the impact of complex matrices on NP behavior using environmentally realistic NP concentrations.

Abbreviations

AF	accumulation factor
CM	culture media
COD	chemical oxygen demand
DLS	dynamic light scattering
dw	dry weight
ELS	electrophoretic light scattering
ICP-MS	inductively coupled plasma - mass spectrometry
MQ	ultra pure water
NM	nanomaterial
NOM	natural organic matter
NP	nanoparticle
PVP	polyvinylpyrrolidone
SI	supporting information
TSS	total suspended solids
UV–Vis	Ultraviolet–visible spectrophotometry
WWTP	wastewater treatment plant
ζ-potential	zeta potential

Funding sources

This study was performed within the Research Council of Norway-funded project ENTRANS (grant agreement number 302378/F20). J. Raths was supported by the Swiss National Science Foundation (200020_184878).

CRediT authorship contribution statement

Sebastian Kuehr: Writing – original draft, Visualization, Methodology, Investigation, Formal analysis, Conceptualization. **Ralf Kaegi:** Writing – original draft, Resources, Methodology, Investigation, Funding acquisition, Conceptualization. **Johannes Raths:** Writing – original draft, Methodology, Investigation. **Brian Sinnet:** Writing – original draft, Methodology, Investigation, Formal analysis. **Marco Kipf:** Writing – original draft, Methodology, Investigation. **Mark Rehkämper:** Writing – original draft, Funding acquisition, Conceptualization. **Karl Andreas Jensen:** Writing – original draft, Methodology, Formal analysis, Conceptualization. **Ralph A. Sperling:** Writing – original draft, Methodology, Formal analysis. **Kuria Ndungu:** Writing – original draft, Funding acquisition, Conceptualization. **Anastasia Georgantzopoulou:** Writing – original draft, Visualization, Resources, Methodology, Funding acquisition, Formal analysis, Conceptualization.

Declaration of competing interest

The authors declare that they have no known competing financial interests or personal relationships that could have appeared to influence the work reported in this paper.

Data availability

Data will be made available on request.

Acknowledgements

The authors thank: S. Richter for assistance during measurement of water parameters. R. Frankhauser and M. Philipp for the technical support during the WWTP spiking experiments. M. Böhler and A. Joss for advice on the operation of the WWTP. J. Hollender for providing *H. azteca* and laboratory equipment for the uptake test performed at Eawag. ARA Neugut-Dübendorf, Switzerland for providing the digested sludge for inoculation of the digester unit. Th. H. Østvedt for assistance with the sample preparation for ICP-MS measurements at NMBU. The graphical abstract and Fig. 1 and S7 were created with *BioRender.com*.

Appendix A. Supplementary data

Supplementary data to this article can be found online at https://doi.org/10.1016/j.scitotenv.2024.174768.

References

Al Aukidy, M., Verlicchi, P., 2017. Contributions of combined sewer overflows and treated effluents to the bacterial load released into a coastal area. Sci. Total Environ. 607–608, 483–496. Dec. https://doi.org/10.1016/j.scitotenv.2017.07.050.

Avellan, A., et al., 2020. Differential reactivity of copper- and gold-based nanomaterials controls their seasonal biogeochemical cycling and fate in a freshwater wetland Mesocosm. Environ. Sci. Technol. 54 (3), 1533–1544. Feb. https://doi.org/10.1021/acs.est.9b05097.

Bastús, N.G., Merkoçi, F., Piella, J., Puntes, V., 2014. Synthesis of highly monodisperse citrate-stabilized silver nanoparticles of up to 200 nm: kinetic control and catalytic

properties. Chem. Mater. 26 (9), 2836–2846. May. https://doi.org/10.1021/CM500316K/SUPPL_FILE/CM500316K_SI_001.PDF.
Benn, T.M., Westerhoff, P., 2008. Nanoparticle silver released into water from commercially available sock fabrics. Environ. Sci. Technol. 42 (11), 4133–4139. https://doi.org/10.1021/es7032718.
Bertinato, J., Cheung, L., Hoque, R., Plouffe, L.J., 2010. Ctr1 transports silver into mammalian cells. J. Trace Elem. Med. Biol. 24 (3), 178–184. Jul. https://doi.org/10.1016/j.jtemb.2010.01.009.
Borgmann, U., 1996. Systematic analysis of aqueous ion requirements of *Hyalella azteca*: a standard artificial medium including the essential bromide ion. Arch. Environ. Contam. Toxicol. 30 (3), 356–363. Mar. https://doi.org/10.1007/BF00212294.
Borgmann, U., Nonvood, W.P., Clarke, C., 1993. Accumulation, regulation and toxicity of copper, zinc, lead and mercury in *Hyalella azteca*. Hydrobiologia 259, 79–89. Accessed: Dec. 08, 2017. [Online]. Available: https://link.springer.com/content/pdf/10.1007%2FBF00008374.pdf.
Bury, N.R., Hogstrand, C., 2002. Influence of chloride and metals on silver bioavailability to Atlantic Salmon (*Salmo salar*) and rainbow trout (*Oncorhynchus mykiss*) yolk-sac fry. Environ. Sci. Technol. 36 (13), 2884–2888. Jul. https://doi.org/10.1021/es010302g.
Cheng, X., et al., 2015. Protein Corona influences cellular uptake of gold nanoparticles by phagocytic and nonphagocytic cells in a size-dependent manner. ACS Appl. Mater. Interfaces 7 (37), 20568–20575. Sep. https://doi.org/10.1021/acsami.5b04290.
Chithrani, B.D., Chan, W.C.W., 2007. Elucidating the mechanism of cellular uptake and removal of protein-coated gold nanoparticles of different sizes and shapes. Nano Lett. 7 (6), 1542–1550. Jun. https://doi.org/10.1021/nl070363y.
Cho, E.C., Xie, J., Wurm, P.A., Xia, Y., 2009. Understanding the role of surface charges in cellular adsorption versus internalization by selectively removing gold nanoparticles on the cell surface with a I_2 /KI etchant. Nano Lett. 9 (3), 1080–1084. Mar. https://doi.org/10.1021/nl803487r.
Derjaguin, B.V., Churaev, N.V., Muller, V.M., 1987. "The Derjaguin - Landau - Verwey - Overbeek (DLVO) Theory of Stability of Lyophobic Colloids," in Surface Forces. Springer, Boston, MA: US, pp. 293–310. https://doi.org/10.1007/978-1-4757-6639-4_8.
Dignac, M.F., Urbain, V., Rybacki, D., Bruchet, A., Snidaro, D., Scribe, P., 1998. Chemical description of extracellular polymers: implication on activated sludge floc structure. Water Sci. Technol. 38 (8–9) https://doi.org/10.1016/S0273-1223(98)00676-3.
Ding, L., et al., 2018. Size, shape, and protein corona determine cellular uptake and removal mechanisms of gold nanoparticles. Small 14 (42), 1801451. Oct. https://doi.org/10.1002/smll.201801451.
Ding, Y., Bai, X., Ye, Z., Gong, D., Cao, J., Hua, Z., 2019. Humic acid regulation of the environmental behavior and phytotoxicity of silver nanoparticles to *Lemna minor*. Environ. Sci. Nano 6 (12), 3712–3722. https://doi.org/10.1039/C9EN00980A.
Evans, D.H., Piermarini, P.M., Choe, K.P., 2005. The multifunctional fish gill: dominant site of gas exchange, osmoregulation, Acid-Base regulation, and excretion of nitrogenous waste. Physiol. Rev. 85 (1), 97–177. Jan. https://doi.org/10.1152/physrev.00050.2003.
García-Negrete, C.A., et al., 2013. Behaviour of au-citrate nanoparticles in seawater and accumulation in bivalves at environmentally relevant concentrations. Environ. Pollut. 174, 134–141. Mar. https://doi.org/10.1016/j.envpol.2012.11.014.
Georgantzopoulou, A., et al., 2018. Ecotoxicological effects of transformed silver and titanium dioxide nanoparticles in the effluent from a lab-scale wastewater treatment system. Environ. Sci. Technol. 52 (16), 9431–9441. Aug. https://doi.org/10.1021/acs.est.0c03113.
Georgantzopoulou, A., et al., 2020. Wastewater-aged silver nanoparticles in single and combined exposures with titanium dioxide affect the early development of the marine copepod *Tisbe battagliai*. Environ. Sci. Technol. 54 (19), 12316–12325. Oct. https://doi.org/10.1021/acs.est.0c03113.
Gottschalk, F., Nowack, B., 2011. The release of engineered nanomaterials to the environment. J. Environ. Monit. 13 (5), 1145. May. https://doi.org/10.1039/c0em00547a.
Gottschalk, F., Sondere, T., Schols, R., Nowack, B., 2009. Modeled environmental concentrations of engineered nanomaterials for different regions. Environ. Sci. Technol. 43 (24), 9216–9222. https://doi.org/10.1021/es9015553.
Hartmann, S., et al., 2019. Comparative multi-generation study on long-term effects of pristine and wastewater-borne silver and titanium dioxide nanoparticles on key lifecycle parameters in *Daphnia magna*. NanoImpact 14, 100163. https://doi.org/10.1016/J.IMPACT.2019.100163.
Harush-Frenkel, O., Debotton, N., Benita, S., Altschuler, Y., 2007. Targeting of nanoparticles to the clathrin-mediated endocytic pathway. Biochem. Biophys. Res. Commun. 353 (1), 26–32. https://doi.org/10.1016/j.bbrc.2006.11.135.
Hogstrand, C., 2003. Internal redistribution of radiolabelled silver among tissues of rainbow trout (*Oncorhynchus mykiss*) and European eel (*Anguilla anguilla*): the influence of silver speciation. Aquat. Toxicol. 63 (2), 139–157. Apr. https://doi.org/10.1016/S0166-445X(02)00174-1.
Hou, J., Wang, X., Hayat, T., Wang, X., 2017. Ecotoxicological effects and mechanism of CuO nanoparticles to individual organisms. Environ. Pollut. 221, 209–217. Feb. https://doi.org/10.1016/j.envpol.2016.11.066.
Hund-Rinke, K., et al., 2021. Nanopharmaceuticals (Au-NPs) after use: experiences with a complex higher tier test design simulating environmental fate and effect. Ecotoxicol. Environ. Saf. 227, 112949. Dec. https://doi.org/10.1016/J.ECOENV.2021.112949.
Inshakova, E., Inshakov, O., 2017. "World market for nanomaterials: Structure and trends," in *MATEC web of conferences*, EDP Sciences, p. 2013. https://doi.org/10.1051/matecconf/201712902013.
Johnson, A.C., Jürgens, M.D., Lawlor, A.J., Cisowska, I., Williams, R.J., 2014. Particulate and colloidal silver in sewage effluent and sludge discharged from British wastewater treatment plants. Chemosphere 112, 49–55. https://doi.org/10.1016/j.chemosphere.2014.03.039.
Kaegi, R., et al., 2011. Behavior of metallic silver nanoparticles in a pilot wastewater treatment plant. Environ. Sci. Technol. 45 (9), 3902–3908. https://doi.org/10.1021/es1041892.
Kaegi, R., et al., 2013. Fate and transformation of silver nanoparticles in urban wastewater systems. Water Res. 47 (12), 3866–3877. Aug. https://doi.org/10.1016/J.WATRES.2012.11.060.
Kampe, S., Kaegi, R., Schlich, K., Wasmuth, C., Hollert, H., Schlechtriem, C., 2018. Silver nanoparticles in sewage sludge: bioavailability of Sulfidized silver to the terrestrial isopod *Porcellio scaber*. Environ. Toxicol. Chem. https://doi.org/10.1002/etc.4102. Jan.
Kuehr, S., 2021. Regulatory bioaccumulation assessment of nanomaterials. Development of new concepts and testing procedures. Universität Siegen. https://doi.org/10.25819/ubsi/9891.
Kuehr, S., Klehm, J., Stehr, C., Menzel, M., Schlechtriem, C., 2020a. Unravelling the uptake pathway and accumulation of silver from manufactured silver nanoparticles in the freshwater amphipod *Hyalella azteca* using correlative microscopy. NanoImpact 19, 100239. Jul. https://doi.org/10.1016/j.impact.2020.100239.
Kuehr, S., Kaegi, R., Maletzki, D., Schlechtriem, C., 2020b. Testing the bioaccumulation potential of manufactured nanomaterials in the freshwater amphipod *Hyalella azteca*. Chemosphere 263, 127961. Jan. https://doi.org/10.1016/j.chemosphere.2020.127961.
Kuehr, S., Kosfeld, V., Schlechtriem, C., 2021a. Bioaccumulation assessment of nanomaterials using freshwater invertebrate species. Environ. Sci. Eur. 33 (1), 1–36. Dec. https://doi.org/10.1186/s12302-020-00442-2.
Kuehr, S., Diehle, N., Kaegi, R., Schlechtriem, C., 2021b. Ingestion of bivalve droppings by benthic invertebrates may lead to the transfer of nanomaterials in the aquatic food chain. Environ. Sci. Eur. 33 (1), 1–16. https://doi.org/10.1186/s12302-021-00473-3.
Kühr, S., Schneider, S., Meisterjahn, B., Schlich, K., Hund-Rinke, K., Schlechtriem, C., 2018. Silver nanoparticles in sewage treatment plant effluents: chronic effects and accumulation of silver in the freshwater amphipod *Hyalella azteca*. Environ. Sci. Eur. 30 (1), 7. Dec. https://doi.org/10.1186/s12302-018-0137-1.
Lee, J., Peña, M.M.O., Nose, Y., Thiele, D.J., 2002. Biochemical characterization of the human copper transporter Ctr1. J. Biol. Chem. 277 (6), 4380–4387. Feb. https://doi.org/10.1074/jbc.M104728200.
Levard, C., Hotze, E.M., Lowry, G.V., Brown, G.E., 2012. Environmental transformations of silver nanoparticles: impact on stability and toxicity. Environ. Sci. Technol. 46 (13), 6900–6914. Jul. https://doi.org/10.1021/es2037405.
Lodeiro, P., Achterberg, E.P., Pampín, J., Affatati, A., El-Shahawi, M.S., 2016. Silver nanoparticles coated with natural polysaccharides as models to study AgNP aggregation kinetics using UV-visible spectrophotometry upon discharge in complex environments. Sci. Total Environ. 539, 7–16. Jan. https://doi.org/10.1016/j.scitotenv.2015.08.115.
Lowry, G.V., Gregory, K.B., Apte, S.C., Lead, J.R., 2012. Transformations of nanomaterials in the Environment. Environ. Sci. Technol. 46 (13), 6893–6899. https://doi.org/10.1021/es300839e.
Ma, R., et al., 2014. Fate of zinc oxide and silver nanoparticles in a pilot wastewater treatment plant and in processed biosolids. Environ. Sci. Technol. 48 (1), 104–112. https://doi.org/10.1021/es403646x.
Mahapatra, I., et al., 2015. Probabilistic modelling of prospective environmental concentrations of gold nanoparticles from medical applications as a basis for risk assessment. J. Nanobiotechnol. 13 (1), 93. Dec. https://doi.org/10.1186/s12951-015-0150-0.
Malvern Panalytical, 2017. "Polydispersity – what does it mean for DLS and chromatography?". Available: https://www.malvernpanalytical.com/de/learn/knowledge-center/insights/polydispersity-what-does-it-mean-for-dls-and-chromatography.
Markus, A.A., Parsons, J.R., Roex, E.W.M., Kenter, G.C.M., Laane, R.W.P.M., 2013. Predicting the contribution of nanoparticles (Zn, Ti, Ag) to the annual metal load in the Dutch reaches of the Rhine and Meuse. Sci. Total Environ. 456–457, 154–160. Jul. https://doi.org/10.1016/J.SCITOTENV.2013.03.058.
Millero, F.J., Feistel, R., Wright, D.G., McDougall, T.J., 2008. The composition of standard seawater and the definition of the reference-composition salinity scale. Deep-Sea Res. I Oceanogr. Res. Pap. 55 (1), 50–72. Jan. https://doi.org/10.1016/j.dsr.2007.10.001.
Muth-Köhne, E., et al., 2013. The toxicity of silver nanoparticles to zebrafish embryos increases through sewage treatment processes. Ecotoxicology 22 (8), 1264–1277. https://doi.org/10.1007/s10646-013-1114-5.
Nativo, P., Prior, I.A., Brust, M., 2008. Uptake and intracellular fate of surface-modified gold nanoparticles. ACS Nano 2 (8), 1639–1644. Aug. https://doi.org/10.1021/nn800330a.
Nowack, B., Bucheli, T.D., 2007. Occurrence, behavior and effects of nanoparticles in the environment. Environ. Pollut. 150 (1), 5–22. Elsevier. Nov. https://doi.org/10.1016/j.envpol.2007.06.006.
OECD Environment Directorate, 2024. "A Tiered Approach for Reliable Bioaccumulation Assessment of Manufactured Nanomaterials in the Environment Whilst Minimising the Use of Vertebrate Testing". In: OECD Series on the Safety of Manufactured Nanomaterials and other Advanced Materials. OECD Series on the Safety of Manufactured Nanomaterials, OECD Publishing, Paris. https://doi.org/10.1787/2f16cda4-en.
Östman, M., Lindberg, R.H., Fick, J., Björn, E., Tysklind, M., 2017. Screening of biocides, metals and antibiotics in Swedish sewage sludge and wastewater. Water Res. 115, 318–328. May. https://doi.org/10.1016/J.WATRES.2017.03.011.

Polesel, F., et al., 2018. Occurrence, characterisation and fate of (nano)particulate Ti and Ag in two Norwegian wastewater treatment plants. Water Res. 141, 19–31. Sep. https://doi.org/10.1016/J.WATRES.2018.04.065.

Poynton, H.C., Chen, C., Alexander, S.L., Major, K.M., Blalock, B.J., Unrine, J.M., 2019. Enhanced toxicity of environmentally transformed ZnO nanoparticles relative to Zn ions in the epibenthic amphipod *Hyalella azteca*. Environ. Sci. Nano 6, 325–340. https://doi.org/10.1039/C8EN00755A.

Quik, J.T.K., Velzeboer, I., Wouterse, M., Koelmans, A.A., van de Meent, D., 2014. Heteroaggregation and sedimentation rates for nanomaterials in natural waters. Water Res. 48, 269–279. Jan. https://doi.org/10.1016/j.watres.2013.09.036.

Rajput, V., et al., 2020. ZnO and CuO nanoparticles: a threat to soil organisms, plants, and human health. Environ. Geochem. Health 42 (1), 147–158. Jan. https://doi.org/10.1007/s10653-019-00317-3.

Schlich, K., et al., 2021. Microbial population dynamics in model sewage treatment plants and the fate and effect of gold nanoparticles. Toxics 9 (3), 54. Mar. https://doi.org/10.3390/toxics9030054.

Sheng, G.-P., Yu, H.-Q., Li, X.-Y., 2010. Extracellular polymeric substances (EPS) of microbial aggregates in biological wastewater treatment systems: a review. Biotechnol. Adv. 28 (6), 882–894. Nov. https://doi.org/10.1016/j.biotechadv.2010.08.001.

Shukla, R., Bansal, V., Chaudhary, M., Basu, A., Bhonde, R.R., Sastry, M., 2005. "Biocompatibility of gold nanoparticles and their endocytotic fate inside the cellular compartment: A microscopic overview," *Langmuir*, vol. 21, no. 23. American Chemical Society, pp. 10644–10654, Nov. 08. https://doi.org/10.1021/la0513712.

Sikder, M., Lead, J.R., Chandler, G.T., Baalousha, M., 2018. A rapid approach for measuring silver nanoparticle concentration and dissolution in seawater by UV–vis. Sci. Total Environ. 618, 597–607. Mar. https://doi.org/10.1016/j.scitotenv.2017.04.055.

Sperling, R.A.. "Particle Size Analyzer ('PSA') for ImageJ." [Online]. Available: https://github.com/psa-rs/psa-macro/pulse.

Stakenborg, T., et al., 2008. Increasing the stability of DNA-functionalized gold nanoparticles using mercaptoalkanes. J. Nanopart. Res. 10 (S1), 143–152. Dec. https://doi.org/10.1007/s11051-008-9425-9.

Stuart, E.J.E., Rees, N.V., Cullen, J.T., Compton, R.G., 2013. Direct electrochemical detection and sizing of silver nanoparticles in seawater media. Nanoscale 5 (1), 174–177. https://doi.org/10.1039/C2NR33146B.

Sun, T.Y., Mitrano, D.M., Bornhöft, N.A., Scheringer, M., Hungerbühler, K., Nowack, B., 2017. Envisioning Nano release dynamics in a changing world: using dynamic probabilistic modeling to assess future environmental emissions of engineered nanomaterials. Environ. Sci. Technol. 51 (5), 2854–2863. Mar. https://doi.org/10.1021/acs.est.6b05702.

Sundara Kumar, K., Sundara Kumar, P., Ratnakanth Babu, M.J., 2010. Performance evaluation of waste water treatment plant. Int. J. Eng. Sci. Technol. 2 (12), 7785–7796. ISSN: 0975-5462.

Surette, M.C., Nason, J.A., Kaegi, R., 2019. The influence of surface coating functionality on the aging of nanoparticles in wastewater. Environ. Sci. Nano 6 (8), 2470–2483. https://doi.org/10.1039/C9EN00376B.

Surette, M.C., McColley, C.J., Nason, J.A., 2021. Comparing the fate of pristine and wastewater-aged gold nanoparticles in freshwater. Environ. Sci. Nano 8 (4), 1109–1120. https://doi.org/10.1039/D1EN00156F.

Tan, Z., et al., 2023. Insight into the formation and biological effects of natural organic matter corona on silver nanoparticles in water environment using biased cyclical electrical field-flow fractionation. Water Res. 228, 119355. Jan. https://doi.org/10.1016/j.watres.2022.119355.

Tayeb, A., Chellali, M.R., Hamou, A., Debbah, S., 2015. Impact of urban and industrial effluents on the coastal marine environment in Oran, Algeria. Mar. Pollut. Bull. 98 (1–2), 281–288. Sep. https://doi.org/10.1016/j.marpolbul.2015.07.013.

Toncelli, C., et al., 2017. Silver nanoparticles in seawater: a dynamic mass balance at part per trillion silver concentrations. Sci. Total Environ. 601–602, 15–21. Dec. https://doi.org/10.1016/j.scitotenv.2017.05.148.

Wang, J., Wang, W., 2014. Salinity influences on the uptake of silver nanoparticles and silver nitrate by marine medaka (*Oryzias melastigma*). Environ. Toxicol. Chem. 33 (3), 632–640. Mar. https://doi.org/10.1002/etc.2471.

Weigel, S., Berger, U., Jensen, E., Kallenborn, R., Thoresen, H., Hühnerfuss, H., 2004. Determination of selected pharmaceuticals and caffeine in sewage and seawater from Tromsø/Norway with emphasis on ibuprofen and its metabolites. Chemosphere 56 (6), 583–592. Aug. https://doi.org/10.1016/j.chemosphere.2004.04.015.

Wielinski, J., Gogos, A., Voegelin, A., Müller, C.R., Morgenroth, E., Kaegi, R., 2021. Release of gold (au), silver (ag) and cerium dioxide (CeO_2) nanoparticles from sewage sludge incineration ash. Environ. Sci. Nano 8 (11), 3220–3232. https://doi.org/10.1039/D1EN00497B.

Wimmer, A., Markus, A.A., Schuster, M., 2019. Silver nanoparticle levels in river water: real environmental measurements and modeling approaches - a comparative study. Environ. Sci. Technol. Lett. 6 (6), 353–358. https://doi.org/10.1021/acs.estlett.9b00211.

Wimmer, A., et al., 2020. What happens to silver-based nanoparticles if they meet seawater? Water Res. 171, 115399. Mar. https://doi.org/10.1016/j.watres.2019.115399.

Zeng, J., et al., 2016. Composition and aggregation of extracellular polymeric substances (EPS) in hyperhaline and municipal wastewater treatment plants. Sci. Rep. 6 (1), 26721. May. https://doi.org/10.1038/srep26721.

Zeumer, R., et al., 2020a. Chronic effects of wastewater-borne silver and titanium dioxide nanoparticles on the rainbow trout (*Oncorhynchus mykiss*). Sci. Total Environ. 723 https://doi.org/10.1016/j.scitotenv.2020.137974.

Zeumer, R., Hermsen, L., Kaegi, R., Kühr, S., Knopf, B., Schlechtriem, C., 2020b. Bioavailability of silver from wastewater and planktonic food borne silver nanoparticles in the rainbow trout *Oncorhynchus mykiss*. Sci. Total Environ. 706, 135695. Nov. https://doi.org/10.1016/J.SCITOTENV.2019.135695.